Journal of Superconductivity: Incorporating Novel Magnetism, Vol. 16, No. 1, February 2003 (© 2003)

Solid-State Silicon NMR Quantum Computer

E. Abe,[1] K. M. Itoh,[1] T. D. Ladd,[2] J. R. Goldman,[2] F. Yamaguchi,[2] and Y. Yamamoto[2]

Received September 30, 2002

A solid-state quantum computer composed entirely of semiconductor silicon is proposed. Qubits are nuclear spins, I = 1/2, of ^{29}Si stable isotopes in the form of atomic chains embedded in a nuclear-spin free matrix of ^{28}Si stable isotopes. Each ^{29}Si nuclear spin in a chain can be accessed selectively with a different resonant frequency (rf) due to a large magnetic field gradient created by a nearby micromagnet, i.e., unitary operations needed for quantum computing can be performed by fine tuning of the rf. Ensemble readout of qubits from 10^5 copies of the atomic chain is accomplished by magnetic resonance force microscopy.

KEY WORDS: solid-state quantum computer; silicon; nuclear spin; ensemble measurement; isotope.

Recent theoretical development of quantum information theory, especially the invention of Shor's factoring alogorithm [1], has spurred physical realization of quantum computers. So far, the only physical system that has succeeded in the experimental implementations of nontrivial quantum algorithms is liquid-state nuclear spin resonance (NMR) at room temperature [2,3]. These solution NMR quantum computers deal with a large ensemble of about 10^{18} nuclear spins of uncoupled, identical molecules. This allows one to control and measure qubits without destroying their coherence or performing single-spin detection. The drawback is that it tends to suffer exponential decrease of signal as adding qubits, because the experiments start with very small nuclear polarization at the thermal equilibrium state of about 10^{-5}. This limits the number of qubits accessible with solution NMR to about 10 qubits [4]. Thus the initialization problem should be addressed in order to improve the scalability of NMR-based quantum computation. The present paper introduces a new NMR quantum computer made exclusively of solid-state silicon (thus named "all-silicon quantum computer") with possibility of a strong nuclear polarization enhancement leading to much improved scalability [5].

[1]Department of Applied Physics and Physico-Informatics and CREST-JST, Keio University, Yokohama 223-8522, Japan.
[2]Quantum Entanglement Project, ICORP, JST Edward L. Ginzton Laboratory, Stanford University, California, 94305-4085.

Figure 1 shows the structure of our all-silicon quantum computer. Qubits are one-dimensional atomic chains of ^{29}Si (spin-1/2) stable isotopes embedded in ^{28}Si (spin-0) stable isotope matrix aligned along the $(1\bar{1}0)$ direction, which we define as the z direction. Nuclear spins in a chain have different resonant frequencies due to a large field gradient from a nearby dysprosium (Dy) micromagnet. Each atomic chain corresponds to each molecule in solution NMR. The magnetic field gradient in our configuration can be as large as $\sim$1.4 T/μm along the z direction [6], i.e., each qubit (each ^{29}Si isotope in a chain) feels different magnetic field from others. A frequency difference between adjacent qubits estimated by $\Delta\omega = \alpha\gamma\partial B^z/\partial z$, is $2\pi \times 2$ kHz, where $\alpha = 0.19$ nm is the projection to the z direction of the distance between two adjacent ^{29}Si nuclei and $\gamma = 2\pi \times 8.46$ MHz/T is the gyromagnetic ratio of ^{29}Si nucleus. The field homogeneity in the xy plane is kept only in a narrow region of 100 μm by 0.2 μm, in which 10^5 atomic chains are placed. Nuclei with identical resonant frequency exist in the same xy plane. The number of identical nuclear spins is so small that the conventional pickup coil could never be used for the detection. Thus, we employ an alternative method for ensemble readout, magnetic resonance force microscopy (MRFM), which is by far the most sensitive NMR method available today [7]. To perform MRFM, ^{28}Si matrix itself forms a high-Q cantilever sustained at both edges, called a "bridge."

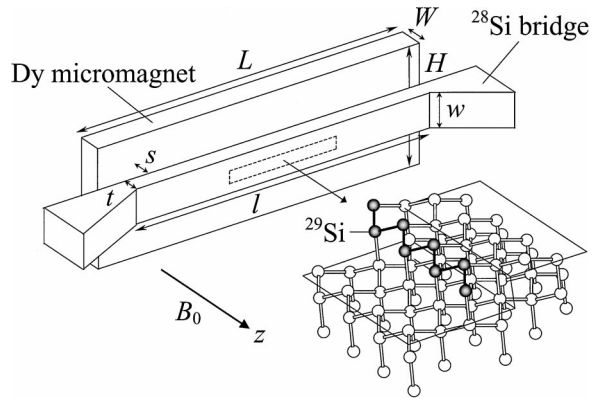

Fig. 1. The integrated bridge and micromagnet structure. The bridge has length $l = 300$ μm, width $w = 4$ μm, and thickness $t = 0.25$ μm. The micromagnet, separated from the bridge with the spacing $s = 2.1$ μm, has length $L = 400$ μm, width $W = 4$ μm, and height $H = 0.25$ μm. The dashed lines represent the active region of 100 μm by 0.2 μm, where atomic chains are embedded. The inset shows the ^{29}Si nuclei aligned at the terrace edge. The aspect ratios are exaggerated. The stucture is kept in high vacuum ($< 10^{-5}$ torr) and at low temperatures ($\sim$4 K). An optical fiber and an rf coil are not shown.

One of the key factors to realize this scheme is engineering of semiconductor isotopes. Natural silicon is composed of three stable isotopes: 92.23% of ^{28}Si, 4.67% of ^{29}Si, and 3.10% of ^{30}Si. Only ^{29}Si has spin 1/2. The growth of isotopically enriched ^{28}Si (99.92%) bulk single crystal has been realized by the present group [8], and the crystal growth of ^{28}Si or other isotopes with higher isotope purity is in process. Another key factor is surface engineering of silicon in order to construct atomically straight chains of ^{29}Si on a surface of a ^{28}Si wafer. It has been reported that highly regular arrays of steps with the average width of 15 nm can be produced on vicinal Si(111)-(7×7) surfaces [9]. Using such materials and techniques, MBE deposition of ^{29}Si in the step-flow mode on atomically straight $(1\bar{1}0)$ terrace edges of a ^{28}Si(111) wafer will allow for the fabrication of atomic chains. The monolithic fabrication of the bridge-shaped silicon cantilever and Dy micromagnet is well within the reach of current technologies.

For initialization, a combination of optical pumping, algorithmic cooling, and pseudo-pure state techniques may be used. Optical pumping is well-known as the powerful method for dynamic nuclear polarization in direct band gap semiconductors like GaAs. Spin-polarized conduction electrons pumped by circularly polarized light interact with host nuclei via hyperfine couplings, which makes the nuclear polarization far beyond the thermal equilibrium possible. After the recombination of photoexcited electrons, no spurious spin that leads to decoherence exists, which is well suited for our purpose, because the isolation of qubits from their environment is achieved during the computation. The nuclear polarization of more than 10% can be achieved for bulk GaAs [10]. However, the polarization enhancement of only 0.1% has been reported for silicon at 77 K in low fields of about 0.1 mT [11]. This low polarization is mainly attributed to the lifetime of photoexcited electrons which is much longer than the electron spin relaxation time. Thus the conduction electrons are only slightly spin polarized. The selection rule of the interband transition, which is different from that of GaAs, also limits the possible electron spin polarization. On the other hand, higher polarization may be achieved for silicon at lower temperatures ($\sim$4 K) and in higher fields ($\sim$10 T). It needs to be tested in the future.

The algorithmic cooling technique redistributes the entropy of a subsystem to another, while preserving the total entropy [12]. The number of pure qubits available from mixed initial n_0 qubits is $[1 - H((1 + p_0)/2)]n_0$, if the procedure is continued to the entropy bound. Here $H(p) = -p \log_2 p - (1 - p) \log_2(1 - p)$ is the entropy function and p_0 is the polarization before the procedure. There are $n_0 = t/a \approx 10^3$ qubits in a chain, hence, to obtain 10^2 clean qubits for instance, the polarization of about 40% is needed before the procedure, i.e., by optical pumping. However, if the polarization is not so large, pseudo-pure state techniques can be applied as in solution NMR case.

MRFM readout is performed using cyclic adiabatic inversion [13]. Suppose we want to detect the ensemble average of a signal arising from a group of ith qubits, which feel the identical static magnetic field B_i^z. In other words, a group of ith qubits are contained in the ith xy plane. The z component of the magnetic force due to the field gradient is given by $F_i^z = M_i^z \partial B^z / \partial z$, where M_i^z is the z component of the ith plane's magnetization. When the alternating magnetic field $B_{\rm rf}$ generated from a coil is applied, the magnetic moment experiences the effective magnetic field given by $B_{\rm eff} = B_{\rm rf}\hat{\mathbf{x}} + (B^z - \omega/\gamma)\hat{\mathbf{z}}$ in the rotating frame, where ω and $B_{\rm rf}$ are the frequency and amplitude of the applied rf field, respectively. If the adiabatic condition $|\omega_m|^2 \ll \gamma B_i^z \Omega$ is satisfied, the magnetization "follows" the effective magnetic field. So the periodic modulation of ω around the ith plane's resonant frequency, in the form $\omega = \gamma B_i^z + \Omega \cos(\omega_m t)$, will cause the oscillating magnetic force, which makes the cantilever oscillate back and forth. Here Ω is the amplitude of frequency modulation and

ω_m is the modulation frequency chosen to be near the mechanical eigen frequency of the bridge. The condition $\Omega \ll \Delta\omega$ must be satisfied, otherwise the adjacent planes would be affected. The phase of the oscillation will differ by π depending on if the spins are up or down. The bridge oscillation can be monitored using an optical-fiber based displacement sensor. In this way, the detection of the signal from the single plane is possible, and simultaneous detection of signals from multiple planes is also possible if the modulation frequencies differ plane by plane. The signals from different planes can be distinguished by the Fourier transform of the oscillation pattern.

Qubits interact via dipolar coupling and their manipulations are accomplished with rf pulse sequences. Such manipulation based on rf pulses are highly established in usual NMR experiments. The dipolar Hamiltonian which couples ith and jth spins within one chain is written [14]

$$\hat{\mathcal{H}}_{ij} = \frac{\mu_0}{4\pi}\gamma^2\hbar^2\frac{1-3\cos^2\theta_{ij}}{r_{ij}^3}\hat{I}_i^z\hat{I}_j^z \qquad (1)$$

where r_{ij} is the length of the vector connecting the spins and θ_{ij} is its angle with the applied field. Especially $\theta_{i,i+1}$ satisfies $\cos^2\theta_{i,i+1} = 2/3$. In NMR quantum computation, it is not easy to exclusively manipulate interaction between spins of two arbitrarily chosen qubits since interactions between other qubits always exist. Therefore proper pulse sequences for coupling selected spins while decoupling others must be applied simultaneously. So called broadband WAHUHA pulses and narrowband Hadamard pulses serve this purpose [15,16]. There remain uncontrollable dipolar couplings even after such pulses are applied. These residual couplings occur between ith and jth planes' nuclei in different chains when ith and jth qubits are coupled. They may cause gate errors, but the error rate can be kept as low as 10^{-6} by using bit-swapping. The possible number of logic gates can be calculated from the decoherence time T_2 divided by the clock speed t_c. The clock speed of this computer is mainly influenced by the size of the Hadamard pulse sequence, which becomes longer as the number of qubits increases [16]. However, not all qubits have to be decoupled because Eq. (1) tells us that couplings between distant qubits are quite small. As a result, the size of the pulse sequence can be optimized, and if sufficiently long T_2 is achieved, our scheme may allow for more than a thousand logic gates.

The scalability of our scheme can be estimated from the viewpoint of SNR. The thermal fluctuation of the bridge (i.e., noise) determines the force resolution for MRFM, while the force from the bridge (i.e., signal) depends on how many nuclei are effectively available. The force from the effective subensemble of nuclei in the pseudo-pure state is estimated as [4]

$$F^z = \frac{\hbar\Delta\omega}{2a}N\left[\left(\frac{1+p}{2}\right)^n - \left(\frac{1-p}{2}\right)^n\right], \qquad (2)$$

where p is the polarization after optical pumping and algorithmic cooling, n is the number of available qubits, and $N = 10^5$ is the number of qubit copies. The minimum detectable force of the bridge in a bandwidth B is estimated by the following equation [17]

$$F_{\min} = \sqrt{\frac{4kk_BTB}{\omega_c Q}}, \qquad (3)$$

where k is a spring constant, ω_c is a resonance frequency, and Q is a quality factor. A lumped harmonic oscillator model yields $k \approx 0.0042$ N/m and $\omega_c \approx 2\pi \times 23$ kHz. We assume a modest value 10^4 for Q. The field homogeneity in a plane gives an estimated value 0.6 kHz for B. The condition that the measurable force exceeds the thermal noise threshold may give the number of available qubits. Evaluating F^z and $F_{\min}$, the number of available qubits as a function of p is plotted in Fig. 2. At low p, exponential improvements in p are needed to increase the number of measurable qubits n. Once p exceeds about 60%, however, n scales as $n \sim (1+p)/(1-p)$, escaping the exponential downscaling which solution NMR suffers. Our estimate shows that if sufficiently high

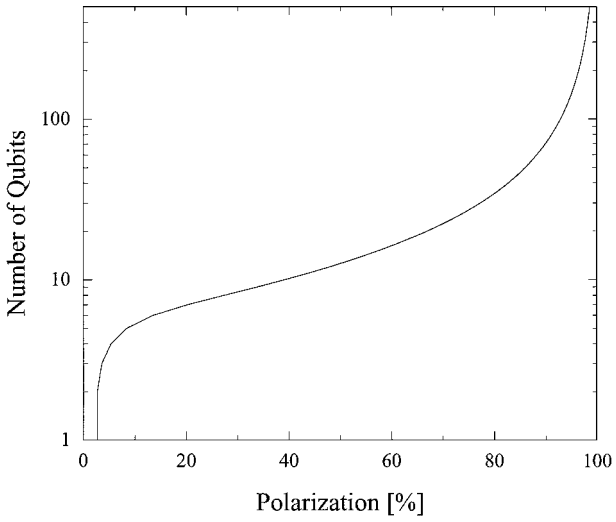

Fig. 2. The number of qubits n as a fuction of the polarization p.

polarizations are achieved, the scheme affords more than a hundred qubits without the need of single-spin detection or unrealistic advances in fabrication, measurement, or control technologies.

ACKNOWLEDGMENTS

The work at Stanford was partially supported by NTT Basic Research Laboratories. T. D. L. was supported by the Fannie and John Hertz Foundation.

REFERENCES

1. P. W. Shor, *SIAM J. Comput.* **26,** 1484 (1997).
2. N. A. Gershenfeld and I. Chuang, *Science*, **275,** 350 (1997); D. G. Cory, A. F. Fahmy, and T. F. Havel, *Proc. Natl. Acad. Sci. USA* **94,** 1634 (1997).
3. L. M. K. Vandersypen, M. Steffen, G. Breyta, C. S. Yannoni, M. H. Sherwood, and I. L. Chuang, *Nature* **414,** 883 (2001), and references therein.
4. W. S. Warren, *Science* **277,** 1688 (1997).
5. T. D. Ladd, J. R. Goldman, F. Yamaguchi, Y. Yamamoto, E. Abe, and K. M. Itoh, *Phys. Rev. Lett.* **89,** 017901 (2002).
6. J. R. Goldman, T. D. Ladd, F. Yamaguchi, and Y. Yamamoto, *Appl. Phys. A* **71,** 11 (2000).
7. J. A. Sidles, J. L. Garbini, K. J. Bruland, D. Rugar, O. Zuger, S. Hoen, and C. S. Yannoni, *Rev. Mod. Phys.* **67,** 249 (1995), and references therein.
8. K. Takyu, K. M. Itoh, K. Oka, N. Saito, and V. I. Ozhogin, *Jpn. J. Appl. Phys.* **38,** L1493 (1999).
9. J. Viernow, J.-L. Lin, D. Y. Petrovykh, F. M. Leibsle, F. K. Men, and F. J. Himpsel, *Appl. Phys. Lett.* **72,** 948 (1998); J.-L. Lin, D. Y. Petrovykh, J. Viernow, F. K. Men, D. J. Seo, and F. J. Himpsel. *J. Appl. Phys.* **84,** 255 (1998).
10. R. Tycko and J. A. Reimer, *J. Phys. Chem.* **100,** 13240 (1996).
11. G. Lampel, *Phys. Rev. Lett.* **20,** 491 (1968).
12. L. J. Schulman and U. V. Vazirani, *in Proceedings of the 31st ACM Symposium on Theory of Computing*, 1999, p. 322; D. E. Chang, L. M. K. Vandersypen, and M. Steffen, *Chem. Phys. Lett.* **338,** 337 (2001).
13. D. Rugar, O. Zuger, S. Hoen, C. S. Yannoni, H.-M. Vieth, and R. D. Kendrick, *Science*, **264,** 1560 (1994).
14. A. Abragam, *Principles of Nuclear Magnetism* (Oxford University Press, New York, 1961).
15. M. Mehring, *High Resolution NMR in Solids* (Springer-Verlag, Berlin, 1983).
16. D. W. Leung, I. L. Chuang, F. Yamaguchi, and Y. Yamamoto, *Phys. Rev. A* **61,** 042310 (1999).
17. J. A. Sidles and D. Rugar, *Phys. Rev. Lett.* **70,** 3506 (1993); T. D. Stowe, K. Yasumura, T. W. Kenny, D. Botkin, K. Wago, and D. Rugar, *Appl. Phys. Lett.* **71,** 288 (1997).